DMD Fast Forward. Published on December 18, 2006 as doi:10.1124/dmd.106.012518




**Characterization of the hepatic disposition of lanoteplase, a rationally designed variant of tissue plasminogen activator, in rodents**

Kazumi Komoriya, Yukio Kato, Yujiro Hayashi, Kazuhiro Ohsuye, Ryuichiro Nishigaki and Yuichi Sugiyama*

Department of Business Planning & Development, Daiichi Asubio Pharma Co., Ltd. 13-1 Takara-machi, Minato-ku, Tokyo 107-8541, Japan (K.K.), Department of Molecular Pharmacokinetics, Graduate School of Pharmaceutical Sciences, University of Tokyo, 7-3-1 Hongo, Bunkyo-ku, Tokyo 113-0033, Japan (Y.K., Y.S.), Institute for Medicinal Research & Development, Daiichi Asubio Pharma Co., Ltd. 2716-1 Kurakake, Akaiwa, Chiyoda-machi, Ohra-gun, Gumma 107-8541, Japan (Y.H., K.O.) and Department of Pharmacokinetics and Biopharmatics, Faculty of Pharmaceutical Sciences, Toho University, 2-2-1 Miyama, Funabashi, Chiba 274-0072, Japan (R.N).

* To whom correspondence should be addressed. (e-mail:sugiyama@mol.f.u-tokyo.ac.jp)

DMD Fast Forward. Published on December 18, 2006 as DOI: 10.1124/dmd.106.012518
This article has not been copyedited and formatted. The final version may differ from this version.



**Running title:** Tissue distribution kinetics of the t-PA variant, lanoteplase

**Corresponding author:**

Prof. Yuichi Sugiyama, Ph.D

Graduate School of Pharmaceutical Sciences, University of Tokyo,

7-3-1 Hongo, Bunkyo-ku, Tokyo 113-0033, Japan.

Tel:(81)-3-5841-4770/Fax:(81)-3-5841-4766/Email: sugiyama@mol.f.u-tokyo.ac.jp

**Document statistics:**

number of text pages: 37

number of tables: 1

number of figures: 5

number of references: 40

number of words:

Abstract: 232

Introduction: 653

Discussion: 1145

**Abbreviations:** t-PA, tissue-type plasminogen activator; AUC, area under the plasma concentration-time curve; $CL_{tot}$, total body clearance; $CL_{uptake}$, tissue uptake clearance; RME, receptor-mediated endocytosis; LRP, low-density lipoprotein receptor-related protein; ASGP, asialoglycoproteins; $k_{off}$, dissociation rate constant of ligand receptor complex; $k_{int}$, internalization rate constant of ligand receptor complex; $k_{deg}$, degradation rate constant of ligand receptor complex

DMD Fast Forward. Published on December 18, 2006 as DOI: 10.1124/dmd.106.012518
This article has not been copyedited and formatted. The final version may differ from this version.



## Abstract

Lanoteplase is a recombinant mutant of tissue-type plasminogen activator (t-PA) that was developed with an aim to overcome the drawback of rapid systemic elimination of t-PA. In this study, we examined the disposition profile of lanoteplase *in vivo* and the kinetics of receptor-mediated endocytosis (RME) of this recombinant t-PA *in vitro* in order to kinetically characterize the mechanism(s) underlying its tissue distribution and elimination. Integration plot analysis of the initial-phase tissue distribution in rats revealed a much lower uptake clearance ($CL_{uptake}$) of lanoteplase in the liver than that of t-PA. Rate constants for cell-surface binding, internalization and degradation of lanoteplase were also lower than those for t-PA in primary cultured rat hepatocytes. These results suggest that the improved stability of lanoteplase *in vivo* could be accounted for by the delay in the RME of this recombinant protein. The $CL_{uptake}$ in the liver decreased with co-administration of lactoferrin, a ligand for the low-density lipoprotein receptor-related protein (LRP) and the asialoglycoprotein (ASGP) receptors in normal mice, and in *lrpap1*$^{(-/-)}$ mice, which have a hereditary deficiency of LRP; In contrast, $CL_{uptake}$ was not affected by mannose, whereas that of t-PA decreased with both ligands and in the *lrpap1*$^{(-/-)}$mice. Thus, the hepatic disposition of lanoteplase appears to be mediated by common specific receptors for t-PA, including LRP and the ASGP receptors, whereas the mannose receptor appears to be only minimally involved in the

disposition of lanoteplase.

## Introduction

Tissue-type plasminogen activator (t-PA) is a serine protease composed of 527 amino acids, containing five structural domains (the finger domain, the EGF domain, the kringle 1 domain, the kringle 2 domain and the serine protease domain) and three sugar chains at amino acid positions 117, 184 and 448. Because of its potent thrombolytic activity, wild-type t-PA has been widely used as a therapeutic thrombolytic agent for myocardial infarction (Llevadot et al., 2001; Collen et al., 2004), and has recently been approved for the treatment of stroke. However, even in such emergent clinical care situations, t-PA must be administered by intravenous infusion because of its short half-life of 3-4 min. Consequently, several types of recombinant t-PA proteins have been developed to prolong the plasma retention time and thereby make a rapid bolus administration of t-PA possible.

Lanoteplase is one of the mutant forms of t-PA, which was developed with the recombinant DNA technology to achieve such an aim. Lanoteplase was produced by removing the EGF domain, a part of the finger domain, and by substituting Gln for the Asn residue at position 117 resulting in a removal of the sugar chain. Despite such a major structural modification, lanoteplase still exhibited a potent thrombolytic activity at much lower dose than t-PA both *in vivo* and in a rabbit model of jugular vein thrombosis (Furuya et al., 1999). In addition, the efficiency of uptake by the liver of

lanoteplase was much lower than that of t-PA, resulting in its longer plasma half-life and lower systemic clearance than those of t-PA (Hata et al., 1997a, Hata et al., 1997b, Larsen et al., 1989). The lower plasma clearance of lanoteplase, compared with t-PA, has also been confirmed in patients with acute myocardial infarction (Kostis et al., 2002). Thus, lanoteplase is expected to become a therapeutic thrombolytic agent, although its pharmacokinetic properties still remain uncertain.

Meanwhile, the clearance via receptor-mediated endocytosis (RME), in which protein ligands are internalized via receptors on the cell surface, subsequently lysosomal degradation is induced, has been recognized as an important mechanism for the systemic elimination of many bioactive proteins, including certain types of cytokines (Sugiyama et al., 1989; Liu et al., 1992; Kuwabara et al., 1996; Tang et al., 2004). In fact, numerous studies have suggested that the low-density lipoprotein receptor-related protein (LRP) receptor, the asialoglycoprotein (ASGP) receptor and the mannose receptor presented on the liver cell-surface might play important roles as clearance mechanisms for t-PA (Camani et al., 1994). Furthermore, Bu et al have suggested that the plasma proteins such as the plasminogen activator inhibitor (PAI)-1 are also associated with such receptor binding (Bu et al., 1992; Otter et al., 1992; Camani et al., 1994). While pharmacokinetic analyses have been performed for various types of recombinant mutant t-PAs, only the plasma elimination profiles have been investigated

in most of those studies (Kuiper at al., 1995; Kuiper at al., 1996; Aoki et al., 2000; Aoki et al., 2001). It is noteworthy that Oikawa et al (2000a, 2000b) attempted to characterize the kinetics of RME in the hepatocytes for pamiteplase, one of the mutant t-PAs, but the elimination mechanism of pamiteplase still remains unclear. The plasma level of t-PA mutants would be expected to be governed by the balance between the administration rate and the elimination efficiency. Therefore, it would be important to elucidate the elimination mechanism of these mutant proteins to clearly understand their pharmacology *in vivo*.

In the present study, we attempted to kinetically characterize the hepatic elimination mechanism of lanoteplase as compare with that of t-PA to elucidate the differences in the elimination pathways between two proteins. First, we performed integration plot analyses to assess their hepatic influx process in rats *in vivo*. Second, we characterized the RMEs of two proteins in primary cultures of rat hepatocytes. Finally, we conducted the inhibition studies about the hepatic uptake, and pharmacokinetic analysis in gene-knockout mice to analyze the hepatic uptake mechanism of those proteins.

## Materials and Methods

**Materials.** Lanoteplase was produced by gene-recombination technology at the production technology laboratories, Suntory Co. Ltd (Daiichi Asubio Pharma Co, Ltd. at present). Wild-type t-PA was purchased from Boehringer Ingelheim Pharma GmbH & Co, KG (Biberach, Germany). $^{125}$I-Sodium iodine (644 GBq/mg) was obtained from Amersham Biosciences (Buckinghamshire, UK). All the other materials and regents used were of analytical grade.

**Radiolabeling.** Lanoteplase and t-PA were radiolabeled with $^{125}$I-sodium iodide by the peroxidase method (Miyachi et al., 1972). Briefly, lanoteplase or t-PA dissolved in a buffer containing 50 mM citric acid, 50 mM creatinine, 50 mM histidine and 0.1% Tween 80 (pH4.6) was first loaded on to a Sephadex G50 column (Amersham Biosciences, Sweden), followed by the addition of $^{125}$I-sodium iodide (24 MBq) dissolved in a buffer containing 0.5 M Arginine, 0.4 M sodium acetate (pH 5.6) and 0.3 μg/mL lactoperoxidase (Carbiochem, Darmstadt, Germany). Then, after the addition of 0.02% $H_2O_2$, the column was incubated at 30 $^{o}$C for 5 min, and the $^{125}$I-lanoteplase or $^{125}$I-t-PA fraction was eluted. The specific radioactivity of $^{125}$I-lanoteplase and $^{125}$I-t-PA were 0.2-0.5 and 0.1-0.5 Bq/g, respectively.

DMD Fast Forward. Published on December 18, 2006 as DOI: 10.1124/dmd.106.012518
This article has not been copyedited and formatted. The final version may differ from this version.



**Animals.** Six-week-old male Sprague Dawley rats (190- 240 g) and six-week-old male C57BL/6N Crj mice (16 -20 g) were purchased from Charles River Japan Inc. (Tsukuba, Japan). In addition, six- to eight- week-old male *lrpap1*$^{(-/-)}$ mice (13-14 g) were purchased from Jackson Laboratory (Bar Harbor, Maine).

**Tissue distribution studies in vivo.** $^{125}$I-lanoteplase and $^{125}$I-t-PA (1 μg/kg (0.37 MBq/kg)) with or without unlabeled ligand (100 μg/kg) were dissolved in a solution for injection (50 mM citric acid, 50 mM creatinine, 50 mM histidine and 0.1% Tween 80; pH 7.6) and injected via the femoral vein into rats under light pentobarbital (Dainippon Pharmaceuticals Co. LTD., Japan) anesthesia (40 mg/kg i.p.). Blood samples were then collected from the femoral artery at designated times for 10 min. Meanwhile, biopsy samples of the liver (approximately 100 mg) were obtained at 1.5, 3, 5 and 7 min after the injection. At 10 min after the i.v. administration, the rats were sacrificed, and the liver, kidney, heart, spleen and brain were immediately removed, weighed and the radioactivity counts were conducted with a gamma counter (COBRAII, Packard).

For the next experiment in mice, $^{125}$I-lanoteplase and $^{125}$I-t-PA (1 μg/kg (0.37 MBq/kg)) were administered via the femoral vein into male C57BL/6N Crj mice or male *lrpap1*$^{(-/-)}$ mice under light anesthesia. Blood samples were then collected from the jugular veins of the mice with disposable syringes at designated intervals for 5 min.

The mice were sacrificed, and the liver, kidney, heart, lung, spleen and brain were immediately removed, weighed and radioactivity counts were performed.

Plasma samples were obtained by the addition of 3.8% sodium citrate to the blood specimens from the animals (1:9 vol/vol) and subsequent centrifugation at 8,000 g for 10 min at 4 $^{o}$C. Ice-cold 4% trichloroacetic acid (TCA, 200 μL) was added to 200 μL of the plasma, followed by incubation for 30 min at 4 $^{o}$C and centrifugation at 8,000 g for 30 min at 4 $^{o}$C. Then, the TCA-precipitable radioactivity in the plasma was counted.

**Kinetic analysis for calculation of the total body clearance ($CL_{tot}$) and tissue uptake clearance ($CL_{uptake}$).** The plasma concentration (Cp)-time profiles were fitted to a bi-exponential equation with a nonlinear least-squares method using the MULTI program (Yamaoka et al, 1981). $CL_{tot}$ was calculated as the dose divided by the area under the plasma concentration-time curve (AUC) for an infinite time.

In regard to the hepatic distribution, the initial slope in a plot (designated as an integration plot) of the tissue:plasma concentration ratio (Kp) vs. the AUC/Cp yielded the $CL_{uptake,}$ where AUC was calculated by the use of the trapezoidal rule with extrapolation to the final sampling (Liu et al., 1992). For tissues other than the liver, the Kp at time zero ($Kp_{(0)}$) was assumed to be the same as that in the extracellular space,

which was obtained as the Kp of $^{125}$I-human serum albumin (Liu et al., 1992), and the $CL_{uptake}$ was calculated as $(Kp - Kp_{(0)})/(AUC/Cp)$.

**Primary cultures of rat hepatocytes.** Rat parenchymal cells were isolated by *in situ* perfusion of the liver with collagenase (Tomita, et.al., 1981). Cells were disseminated on a collagen-coated 24-well plate (Sumitomo Bakelite Co. LTD., Japan) containing the culture medium (William's medium E containing 5% calf serum, 1 nM insulin, 1 nM dexamethasone, and 30 mg/L kanamycin monosulphate) at the density of 1.5 x $10^5$ cells/well (0.32 $mm^{-1}$) and incubated for 3 hr in an atmosphere containing 5% $CO_2$ at 37 $^oC$. The cells were washed twice and consecutively cultured for 21 hr under the same conditions. The monolayer formed was then washed with standard medium (Hanks buffer with 20 mM Hepes (pH 7.4) containing 0.2% bovine serum albumin) and preincubated for 30 min before starting the following experiments.

**Binding assay.** After setting the cell plate on the ice, the cells were incubated in the ice-cold standard medium containing $^{125}$I-lanoteplase or $^{125}$I-t-PA (0.1 pmol/0.45 kBq/mL) and various concentrations (0.1-100 nM) of unlabelled ligands for 240 min at 4 $^oC$. The cells were washed, solubilized in 1 N NaOH and their radioactivity count was performed. The binding was calculated as the ratio of the surface-bound amount

thus obtained to the ligand concentration in the medium.

**Determination of surface-binding, internalization and degradation.** The cell monolayer was incubated in standard medium containing $^{125}$I-lanoteplase or $^{125}$I-t-PA (0.1 pmol/0.45 kBq/mL) in an atmosphere containing 5% $CO_2$ at 37 $^{o}$C, and the reaction was terminated by aspiration of the medium at designated times. The monolayer was then washed twice with the ice-cold standard medium, and the washed medium was mixed with the reaction medium aspirated as mentioned above. An aliquot (1 mL) of the mixture was then subjected to the TCA-precipitation technique, and TCA-precipitable (intact) and soluble (degradated) radioactivities were counted (Hata et al., 1997b). In our previous analysis comparing the TCA-precipitation method with gel-filtration, polypeptide with molecular weight of higher than 15 kD was regarded as TCA-precipitable radioactivity (Hata et al., 1997b). In our preliminary study, both $^{125}$I-lanoteplase and $^{125}$I-t-PA were incubated with rat liver homogenate which contains endogenous Type I deiodinase, and time-dependent increases in the TCA-soluble fraction were similar between the two proteins, suggesting that the rate of deionidation of the two proteins is the same. Accordingly, the monolayer was incubated for 20 min at 4 $^{o}$C with the ice-cold acid buffer (Hanks buffer with 20 mM MES and 0.2% BSA; pH 3.0), and washed twice with the same acid buffer (Haigler et al., 1980). The ligand

released in this series of acid-washings was designated as the surface-bound ligand. The monolayer was solubilized by incubation with 0.5 N NaOH for 30 min at 37 $^{o}$C, and washed twice with 0.5 N NaOH. The NaOH-extract thus obtained was regarded as the internalized ligand. Cellular protein was measured by the BioRad protein assay kit using BSA as the standard. All the radioactivities measured were normalized by both the cellular protein and the initial ligand concentration in the medium, and expressed as distribution volume (μL/mg protein).

**Kinetic analysis for receptor-mediated endocytosis.** Regarding the receptor binding on cell-surface, internalization and degradation of the ligand, the following three equations can represent the mass balance in each process:

$$dX_s/dt = k_{on} \bullet L \bullet R_{free} - (k_{off} + k_{int}) \bullet X_s \quad (1)$$

$$dX_{int}/dt = k_{int} \bullet X_s - k_{deg} \bullet X_{int} \quad (2)$$

$$dX_{deg}/dt = k_{deg} \bullet X_{int} \quad (3)$$

where $X_s$, $X_{int}$ and $X_{deg}$ are the amounts of surface-bound, internalized and degraded ligand, respectively, at time t, whereas $k_{on}$, $k_{off}$, $k_{int}$ and $k_{deg}$ indicate the rate constants for association, dissociation, internalization and degradation, respectively. The L and $R_{free}$ are ligand concentration in medium and free (unoccupied) receptor on cell-surface. At the earlier time period, the Eq. 2 can be simplified to:

DMD Fast Forward. Published on December 18, 2006 as DOI: 10.1124/dmd.106.012518
This article has not been copyedited and formatted. The final version may differ from this version.



$$dX_{int}/dt = k_{int} \bullet X_s \quad (4)$$

The integration of Eq. 4 and Eq. 3 yields:

$$X_{int} = k_{int} \bullet AUC_s \quad (5)$$

$$X_{deg} = k_{deg} \bullet AUC_{int} \quad (6)$$

where $AUC_s$ and $AUC_{int}$ are area under the time course of $X_s$ and $X_{int}$, respectively. Thus, initial slope in the plot of $X_{int}$ vs $AUC_s$ yields $k_{int}$ whereas that in the plot of $X_{deg}$ vs $AUC_{int}$ yields $k_{deg}$. Since we used a tracer concentration of the ligand, the $R_{free}$ was assumed to be constant. In addition, L was also assumed to be constant, since the decrease in medium ligand concentration was found to be minimal in the present study. Thus, the Eq. 1 can be simply integrated to be:

$$X_s = \text{Constant} \bullet (1 - \exp(-(k_{off}+k_{int})\, t)) \quad (7)$$

Therefore, the slope in sigma-minus plot for $X_s$ yields sum of $k_{off}$ and $k_{int}$, and subtraction of $k_{int}$ from the slope yields $k_{off}$.

**Statistical Analysis.** Statistical comparisons between the treatment group were performed using one-way analysis of variance (ANOVA). When ANOVA showed significant differences among the groups, multiple pairwise comparisons of each experimental group versus the control group were performed using Dunnett's test to identify which group differences accounted for the significant P values. The p-value

of less than 0.05 with two-tailed was considered statistically significant.

## Results

### Comparison of the disposition profile between $^{125}$I-lanoteplase and $^{125}$I-t-PA in rats.

The plasma concentration-time profiles after i.v. administration of 1 and 100 μg/kg of $^{125}$I-lanoteplase and $^{125}$I-t-PA are shown in Fig. 1. The disappearance of lanoteplase from the plasma was significantly slower than that of t-PA, with the plasma concentration of lanoteplase at 10 min after its administration being about 5-fold higher than that of the corresponding concentration of $^{125}$I-t-PA (Fig. 1).

Since the liver has been considered to be the major clearance organ for t-PA (Camani et al., 1994), the hepatic uptake profile of both lanoteplase and t-PA were examined by the integration plot analysis. The integration plot for the liver was almost linear up to 10 min for both proteins, although the slope for t-PA was much steeper than that for lanoteplase, after administration of either 1 or 100 μg/kg (Fig. 2). The $CL_{uptake}$s in the liver and other organs are shown in Fig. 3. The $CL_{uptake}$s of lanoteplase in the liver, spleen and heart were significantly lower than the corresponding values of t-PA, in particular, that of lanoteplase in the liver was just about 7% of t-PA's (Fig. 3A). Meanwhile, the $CL_{uptake}$ of lanoteplase in the kidney was about 1.6 times higher than that of t-PA (Fig. 3A). In addition, the $CL_{uptake}$ of t-PA per kg body weight in the liver was the highest among all organs examined, whereas those of lanoteplase in the liver and kidney were comparable (Fig. 3B). Furthermore, those of lanoteplase and t-PA in

the liver were around 60% and 89% of the $CL_{tot}$, respectively, showing the consistency with the study results reported by Camani et al. that the major organ of elimination of t-PA from the circulating blood was the liver (Camani et al., 1994). The difference in the $CL_{tot}$ between lanoteplase and t-PA was comparable to the difference in the $CL_{uptake}$ per kg body weight in the liver between the two proteins (Fig. 3B, 3C). Thus, the improved stability in the systemic circulation of lanoteplase as compared with that of t-PA can be principally explained by the lower hepatic elimination of this protein, as hypothesized by us in our previous report (Hata et al., 1997b).

**Kinetic analysis of RME for lanoteplase and t-PA in primary cultures of rat hepatocytes.** To characterize the hepatic disposition mechanism of lanoteplase, we next focused on the kinetics of the hepatocellular handling of the proteins in a primary hepatocyte culture monolayer. The cell-surface binding of both proteins at 4 $^{o}$C, at which temperature endocytosis is normally inhibited, increased to reach equilibrium at around 120 min, with the binding of lanoteplase at this time-point being about 45% of that of t-PA (Fig. 4A). At 37 $^{o}$C, the surface-binding of both proteins increased rapidly within 5 min after the start of incubation, to reach a steady-state at around 30 min (Fig. 4B). The internalization of both proteins at 37 $^{o}$C started to increase rapidly within 20 min, to reach a steady-state at around 120 min (Fig. 4C). Degradation products of both

the proteins were detected after a lag-time (~30 min), the amounts increasing steadily until 240 min (Fig. 4D). The amount of surface-binding, internalization and degradation at 37 $^{o}$C of lanoteplase at 240 min were 57, 48 and 13%, respectively, relative to that of t-PA. The amount of surface-binding at 37 $^{o}$C (Fig. 4B) was lower than that at 4 $^{o}$C (Fig. 4A) for both proteins, probably because of such efficient internalization and subsequent intracellular degradation. To conduct a more quantitative comparison of each process of the RME, kinetic parameters were calculated. The $k_{off}$ of lanoteplase was about three times as high as that of t-PA. On the other hand, the $k_{int}$ and $k_{deg}$ of lanoteplase were only 53 and 36%, respectively, of those of t-PA. Thus, all the three processes of RME, that is, cell-surface binding, internalization and degradation of lanoteplase were slower than those of t-PA (Table 1 ).

**Characterization of the tissue uptake mechanism(s) of lanoteplase in mice.** To analyze the hepatic uptake mechanism for lanoteplase, a tissue distribution study was performed in mice by co-administration of ligands for receptors that have already been suggested to be involved in the uptake of t-PA. Lactoferrin and mannose were used as the ligands for the LRP and the ASGP receptors and for the mannose receptors on liver cells, respectively, the dose of each ligand being set so as to be sufficient to saturate each receptor (180 mg/kg and 120 mg/kg, respectively), based on previous reports

(Brock 1997; Crawford et al., 1999; Emeis et al, 1985). The Kp of lanoteplase in the liver at 3 min after its administration was not affected by the co-administration of mannose, however, it decreased significantly by the co-administration of lactoferrin alone and by the co-administration of lactoferrin plus mannose (Fig. 5A). On the other hand, mannose and/or lactoferrin co-administration decreased the Kp of t-PA in the liver (Fig. 5B). The trend of Kp of lanoteplase in the kidney was similar to that in the liver (Fig. 5A, 5C), whereas that of t-PA in the kidney was not significantly affected by the co-administration of neither mannose, lactoferrin, nor lactoferrin plus mannose (Fig. 5D).

It has been suggested that the hepatic disposition of t-PA was at least partially mediated by the LDL receptor-related protein (LRP) (Bu et al, 1992). The LRP-associated protein (LRPAP in humans, RAP in mice) may act as a folding chaperone for LRP (Willnow et al, 1996) and has been widely used as a specific inhibitor of LRP. Target mutation in the *lrpap1* gene causes functional deficiency of LRP, with reduction in its expression levels in the liver and *lrpap1*$^{(-/-)}$ mice are now commercially available. Therefore, in the present study, *lrpap1*$^{(-/-)}$ mice were used to investigate the possible involvement of LRP in the hepatic disposition of lanoteplase. While the Kp of lanoteplase in the liver tended to be decreased in the *lrpap1*$^{(-/-)}$ mice (Fig. 5A), an obvious decrease of the Kp of t-PA was observed in the liver of these mice

(Fig. 5B).

## Discussion

It has been obligatory to administer t-PA by intravenous infusion in emergency medical situations due to its short half-life (Collen et al., 1984; Verstraete et al., 1985). Lanoteplase is a brand new mutant t-PA produced as a result of a major structural modification with a molecular size $4/5^{th}$ that of t-PA. It has similarly potent thrombolytic activity as t-PA (Furuya et al., 1999) and pharmacokinetic properties that should enable bolus intravenous administration for the treatment of acute emergencies. The present study indicated that the major clearance organ for both t-PA and lanoteplase is the liver (Fig. 3). However, the hepatic $CL_{uptake}$ of lanoteplase was quite smaller than that of t-PA (Fig. 2, 3), and such smaller hepatic uptake could be a reason for the prolonged retention of lanoteplase in the circulating blood.

Previous reports have revealed that about 60% of hepatic distribution of t-PA was associated with parenchymal cells, and the remaining 40% was associated with non-parenchymal cells of the liver (Kuiper at al., 1988; Rijken et al., 1990). The LRP and ASGP receptors on the parenchymal cells and also the mannose receptors on the non-parenchymal cells of the liver could represent the clearance receptors for t-PA on the liver cell-surface (Bu et al., 1992; Otter et al., 1992; Camani et al., 1994). We therefore investigated the RME mechanism for lanoteplase and t-PA in primary cultured rat hepatocytes. The amounts of surface-bound, internalized and degradation products

of lanoteplase were smaller than those of t-PA (Fig. 4B, 4C, and 4D), suggesting that lanoteplase also underwent RME in the parenchymal cells just like t-PA, but its clearance via RME was smaller than that of t-PA. Cell-surface binding of lanoteplase assessed at 4 $^{o}$C was lower than that of t-PA (Fig. 4A), suggesting lower receptor binding affinity of lanoteplase. Furthermore, the kinetic analyses suggested that a reduction in internalization and degradation (Table 1) could also be the reason for lower clearance efficiency of lanoteplase via RME.

It is considered important from a perspective of safety in the clinical use to clarify which ones among the three receptors in the liver cells are responsible for the elimination of lanoteplase. The $CL_{uptake}$ of lanoteplase in the liver was decreased only when co-administered with lactoferin or administered to *lrpap1*$^{(-/-)}$ mice (Fig. 5A), even though that of t-PA decreased when co-administered under the same experimental conditions including mannose (Fig. 5B). These results suggested that the ASGP receptor and the specific receptor for LRPAP, presumably the LRP receptor, were responsible for the distribution of lanoteplase into the liver. Meanwhile, the LRP, the ASGP and the mannose receptors were responsible for the distribution of t-PA into the liver. Based on these results, it is considered that the binding of lanoteplase to the mannose receptor may have completely disappeared because of the removal of the mannose-rich sugar chain from its molecule at Asn 117. This is compatible with the

previous report that the $CL_{tot}$ of another structural mutant of t-PA, in which Asn at 117 was substituted by Gln and a sugar chain was removed, was decreased by 38% of that of t-PA (Aoki et al. 2001) . LRP is known to consist of four clusters, and the t-PA·PAI-1 complex binds to cluster II of LRP (Neels et al., 1999). The binding affinity of t-PA·PAI-1 complex to the LRP receptor is ten times higher than that of non-protein binding (free) t-PA (Horn et al., 1997). Moreover, it has been reported that lactoferrin binds to clusters II and IV of the LRP (Bennatt et al., 1997; McAbee et al., 1998). Considering that the distribution of lanoteplase into the liver was inhibited by co-administration of lactoferrin (Fig. 5), and that lanoteplase was a mutant of t-PA, it would appear that lanoteplase is also taken up by the liver mainly as a protein-bound complex. On the other hand, the ASGP receptor binds to t-PA and this receptor is known to recognize the structural carbohydrates of t-PA at Thr 61, Arg 184, and Asn 448 (Camani et al., 1998; Nagaoka et al., 2003). As the carbohydrate at Asn 448 is also retained in lanoteplase, the drug appears to bind to the ASGP receptor.

It is noteworthy that the $CL_{uptake}$ per g tissue of lanoteplase in the kidney was greater than that in the liver, and that the $CL_{uptake}$ values per kg body weight of this compound in the liver and kidney were comparable (Fig. 3). This result showed that the kidney may also be an important clearance organ for lanoteplase. Hepatic dysfunction may severely affect the pharmacokinetics when the clearance organ is only

the liver, and multiple elimination pathways may be beneficial for the clearance of therapeutic agents. Therefore, further clinical studies are necessary to examine whether lanoteplase might be safer than the traditional t-PA when it is administered to the specific target population such as the patients with hepatic dysfunction, those receiving concomitant estradiol administration or older patients. Until now, there have been few reports about the renal elimination mechanism of t-PA even though it was suggested that t-PA might be taken up by one of the members of LDL receptor family in this organ (Camani et al., 1994). Considering the significance of renal elimination (Fig. 3), it would also be important for lanoteplase to clarify the mechanism of renal elimination in detail. The present study indicated the similar patterns in decrease of the Kp of lanoteplase between kidney and liver (Fig. 5C), implying that RME may also be involved in renal disposition, although the higher $CL_{uptake}$ of lanoteplase in the kidney (Fig. 3) may presumably be explained by the easier glomerular filtration of lanoteplase because of its smaller molecular size (50 kD) than that of t-PA (64 kD).

In our previous study using gel filtration chromatography, the major plasma proteins that bind to t-PA and lanoteplase were different; that is, the binding fractions for t-PA to PAI-1 and α2-macroglobulin were 19 and 8%, whereas the corresponding values for lanoteplase were 6 and 14%, respectively (Hata et al., 1997b). On the other hand, the uptake of t-PA into the liver has been reported to be affected by its binding to

PAI-1 or α2-macroglobulin, presumably because t-PA was taken up into the liver as a complex with these proteins (Camani et al., 1994, Camani et al., 2000). Thus, it is possible that the binding of lanoteplase to the plasma proteins or these receptors is changed because of conformational changes following the removal of several structural domains in t-PA. To conduct an in-depth analysis of the elimination mechanisms, furtherer examination using the protein complexes might be needed.

In conclusion, lanoteplase showed long blood retention mainly because of a decrease in the efficiency of RME in the liver. The primary receptors related to the hepatic uptake for lanoteplase seemed to be the LRP and the ASGP receptors and the contribution of mannose receptor appeared to be small.

## ACKNOWLEDGEMENT

We thank Dr. Ke-Xin Liu (presently in College of Pharmacy, Dalian Medical University) for helpful advice concerning *in vivo* studies. We thank Dr. Takeshi Hanada and Dr. Yasushi Kanai (Daiichi Asubio Pharma Co., Ltd.) for their support during this study.

## References

Aoki S, Shimizu N, Koyama J, Kato Y, Kitagawa M, Okumura K, and Tanigawara Y (2000) Influence of N-terminal peptide and oligosaccharide on the clearance of t-PA. *Biol Pharm Bull* **23**(4)**:**477-481.

Aoki S, Kitagawa M, and Okumura K (2001) Pharmacokinetic studies of Gln117 tissue-type plasminogen activator in rats. *J Pharm Biomed Anal* **26:**453-462.

Bennatt DJ, Ling YY, and McAbee DD (1997) Isolated rat hepatocytes bind lactoferrins by the RHL-1 subunit of the asialoglycoprotein receptor in a galactose-independent manner. *Biochemistry* **36:**8367-8376.

Brock JH (1997) Lactoferrin structure-function relationships. in *Lactoferrin*: *Interactions and biological functions* (Hutchens TW and Lonnerdal B eds) pp3 23,Human Press Totowa, New Jersey.

Bu G, Williams S, Strickland DK, and Schwartz AL (1992) Low density lipoprotein receptor-related protein/α2-macroglobulin receptor is a hepatic receptor for tissue-type plasminogen activator. *Proc Natl Acad Sci USA* **89:**7427-7431.

Camani C and Kruithof EKO (1994) Clearance receptors for tissue-type plasminogen activator. *Int J Hematol* **60:**97-109.

Camani C, Gavin O, Bertossa C, Samatani E, and Kruithof EKO (1998) Studies on the effect of fucosylated and non-fucosylated finger/growth-factor contructs on the

clearance of tissue-type plasminogen activator mediated by the low-density-lipoprotein-receptor-related protein. *Eur J Biochem* **251:**804-811.

Camani C, Gavin O, and Kruithof EKO (2000) Cellular degradation of free and inhibitor-bound tissue-type plasminogen activator. *Thromb Haemost* **83:**290-306.

Collen D and Lijnent HR (2004) Tissue-type plasminogen activator: a historical perspective and personal account. *J Thromb Haemost* **2**: 541–546.

Collen D, Stassen JM, Marafino BJ Jr, Builder S, De Cock F, Ogez J, Tajiri D, Pennica D, Bennett WF, Salwa J, and Hoyng CF (1984) Biological properties of human tissue-type plasminogen activator obtained by expression of recombinant DNA in mammalian cells. *J Pharmacol Exp Ther* **231**(1)**:**146-152.

Crawford SE and Borensztajn J (1999) Plasma clearance and liver uptake of chylomicron remnants generated by hepatic lipase lipolysis: evidence for a lactoferrin-sensitive and apolipoprotein E-independent pathway. *J Lipid Res* **40:**797-805.

Emeis JJ, Van den Hoogen CM, and Jense D (1985) Hepatic clearance of tissue-type plasminogen activator in rats. *Thromb Haemostasis* **54**(3)**:**661-664.

Furuya M, Oka N, Horikawa Y, Ogata A, Inomata N, Ohno T, Timony GA, Bree AG, Stoudemire JB, and Horgan P (1999) Thrombolytic activity in jugular vein thrombosis and bleeding potential of lanoteplase (SUN 9216) in rabbits. *Jpn*

*Pharmacol Ther* **27:**141-150.

Haigler HT, Maxfield FR, Willingham MC, Pastan I (1980) Dansylcadaverine inhibits internalization of 125I-epidermal growth factor in BALB 3T3 cells. *J Biol Chem* **255**: 1239-1241.

Hata K, Komoriya K, Takada N, Kobayashi H, Ohnuma N, and Hayashi Y (1997a) Pharmacokinetic studies of lanoteplase, a novel tissue plasminogen activator (1) plasma levels after a single bolus intravenous administration in rats, rabbits and dogs. *Oyo Yakuri/Pharmacometrics* **53**(1)**:**1-10.

Hata K, Komoriya K, Takada N, Kobayashi H, Ohnuma N, and Hayashi Y (1997b) Pharmacokinetic studies of lanoteplase, a novel tissue plasminogen activator (2) tissue distribution after a single bolus intravenous administration in rats. *Oyo Yakuri/Pharmacometrics* **53**(1)**:**11-21.

Horn IR, Van den Berg BMM, Van der Meijden PZ, Pannekoek H, and Van Zonneveld AJ (1997) Molecular analysis of ligand binding to the second cluster of complement-type repeaters of the low density lipoprotein receptor-related protein. *J Biol Chem* **272(21):**13608-13613.

Kostis JB, Dockens RC, Thadani U, Bethala V, Pepine C, Leimbach W, Vachharajani N, Raymond RH, Stouffer BC, Tay LK, Shyu WC, and Liao WC.(2002) Comparison of pharmacokinetics of lanoteplase and alteplase during acute myocardial infarction.

*Clin Pharmacokinet* **41**(6)**:**445-452.

Kuiper J, Otter M, Rijken DC, and Van Berkel ThJC (1988) Characterization of the interaction in vivo of tissue-type plasminogen activator with liver cells. *J Biol Chem* **263**(34)**:**18220-18224.

Kuiper J, Van de Bilt H, Martin U, and Van Berkel ThJC (1995) Uptake, internalization and degradation of the novel plasminogen activator reteplase(BM 06.022) in the rat. *Thromb Haemostasis* **74**(6)**:**1501-1510.

Kuiper J, Van't Hof A, Otter M, Biessen EAL, Rijken DC, and Van Berkel ThJC (1996) Interaction of mutants of tissue-type plasminogen activator with liver cells: effect of domain deletions. *Biochem J* **313:**775-780.

Kuwabara T, Kobayashi S, and Sugiyama Y (1996) Pharmacokinetics and pharmacodynamics of a recombinant human granulocyte colony-stimulating factor. *Drug Metab Rev* **28**: 625-658.

Larsen GR, Metzger M, Henson K, Blue Y, and Horgan P (1989) Pharmacokinetic and distribution analysis of variant forms of tissue-type plasminogen activator with prolonged clearance in rat. *Blood* **73**(7)**:**1842-1850.

Liu K, Kato Y, Narukawa M, Kim DC, Hanano M, Higuchi O, Nakamura T, and Sugiyama Y (1992) Importance of the liver in plasma clearance of hepatocyte growth factor in rats. *Am J Physiol* **263:**G642-G649.

Llevadot J, Giugliano RP, and Antman EM (2001) Bolus fibrinolytic therapy in acute myocardial infarction. *JAMA* **286**: 442-449.

McAbee DD and Ling YY (1997) Iron-loading of cultured adult rat hepatocytes reversibly enhances lactoferrin binding and endocytosis. *J Cell Physiol* **171:**75-86.

McAbee DD, Bennatt DJ, and Ling YY (1998) Identification and analysis of a $Ca^{2+}$-dependent lactoferrin receptor in rat liver. *Advances in Lactoferrin Research* (Spik et al., ers) pp113-121, Plenum Press, New York.

Miyachi Y, Vaitukaitis JL, Nieschlag E, and Lipsett MB (1972) Enzymatic Radioiodination of Gonadotropins. *J Clin Endocr* **34:**23-28.

Nagaoka MR, Strital E, Kouyoumdjian M, and Borges DR (2003) Participation of a galectin-dependent mechanism in the hepatic clearance of tissue-type plasminogen activator and plasma kallikrein. *Thromb Res* **108:**257-262.

Neels JG, Van den Berg BMM, Lookene A, Olivecrona G, Pannekoek H, and Van Zonneveld AJ (1999) The second and fourth cluster of class A cysteine-rich repeats of the low density lipoprotein receptor-related protein share ligand-binding properties. *J Biol Chem* **274**(44)**:**31305-31311.

Oikawa K, Watanabe T, and Higuchi S (2000a) Comparison of drug disposition between wild-type and novel tissue-type plasminogen activator pamiteplase in rats. *Drug Metab Dispos* **28:**1087-1093.

Oikawa K, Watanabe T, and Higuchi S (2000b) Comparison of Receptor-mediated endocytosis kinetics between wild-type t-PA and recombinant pamiteplase in isolated rat hepatocytes and liver cell plasma membranes. *Xenobiotica* **30**(7)**:**693-705.

Otter M, Kuiper J, Van Berkel ThJC, and Rijken DC (1992) Mechanisms of tissue-type plasminogen activator(t-PA) clearance by the liver *Ann N Y Acad Sci* **667:**431-442.

Rijken DC, Otter M, Kuiper J, and Van Berkel ThJC (1990) Receptor-mediated endocytosis of tissue- type plasminogen activator (t-PA) by liver cells. *Thromb Res* **suppl X:**63-71.

Sugiyama Y and Hanano M (1989) Receptor-mediated transport of peptide hormones and its importance in the overall hormone disposition in the body. *Pharm Res (NY)* **6**(3)**:**192-202.

Tang L, Persky AM, Hochhaus G, and Meibohm B (2004) Pharmacokinetic aspects of biotechnology products. *J Pharm Sci* **93**: 2184-2204.

Tomita Y, Nakamura T, and Ichihara A (1981) Control of DNA synthesis and ornithine decarboxylase activity by hormones and amino acids in primary cultures of adult rat hepatocytes. *Exp Cell Res* **135:**363-371.

Verstraete M, Bounameaux H, de Cock F, Van de Werf F, and Collen D (1985) Pharmacokinetics and systemic fibrinogenolytic effects of recombinant human

tissue-type plasminogen activator (rt-PA) in humans. *J Pharmacol Exp Ther* **235**(2)**:**506-512.

Willnow TE, Rohlmann A, Horton J, Otani H, Braun JR, Hammer RE, and Herz J (1996) RAP, a specialized chaperone, prevents ligand-induced ER retention and degradation of LDL receptor-related endocytic receptors. *EMBO J* **15**(11)**:**2632-2639.

Yamaoka K, Tanigawara Y, Nakagawa T, and Uno T (1981) A pharmacokinetic analysis program (MULTI) for microcomputer. *J Pharmacobio-Dyn* **4:**879-885.

## Legends for Figures

**Fig. 1 Plasma concentration-time profiles of $^{125}$I-lanoteplase (filled circles) or $^{125}$I-t-PA (open circles) after intravenous administration in rats.**

TCA-precipitable radioactivity in the plasma was determined after i.v. administration of $^{125}$I-lanoteplase and $^{125}$I-t-PA at the dose of 1 (A) and 100 μg/kg (B). Each point and vertical bar represent the mean ±S.D. from 3 to 8 animals.

**Fig. 2 Integration plots for estimating the hepatic uptake clearance ($CL_{uptake}$).**

After i.v. administration of $^{125}$I-lanoteplase (filled circles) and $^{125}$I t-PA (open circles) at 1 (A) and 100μg/kg (B), the time-profiles of TCA-precipitable radioactivity in the plasma and radioactivity in the liver were determined for 10 min. The data were expressed as integration plots, the initial slope representing the $CL_{uptake}$.

**Fig. 3 Tissue uptake clearance ($CL_{uptake}$) of $^{125}$I-lanoteplase (filled bars) and $^{125}$I-t-PA (open bars) per g of tissue (A) or per kg body weight (B), and their total body clearance ($CL_{tot}$).**

The $CL_{uptake}$ in the liver was obtained from Fig. 2, whereas that in other tissues was obtained from the time-profiles of the plasma concentrations and Kp at 10 min after i.v. administration. Each point and vertical bar represent the mean ± S.D. from 3 to 8

animals.

**Fig. 4 Time-courses of the surface-binding, internalization and degradation of $^{125}$I-lanoteplase (filled circles) and $^{125}$I-t-PA (open circles) in primary cultures of rat hepatocytes.**

The cells were incubated with a tracer concentration (0.1 nM) of $^{125}$I-lanoteplase or $^{125}$I-t-PA at 4 $^{o}$C (A) or 37 $^{o}$C (B, C, D), and the surface-bound (A, B), internalized (C) and degraded (D) amounts were measured. All these values were normalized by both the cellular protein and the initial ligand concentration in the medium, and expressed as μL/mg protein. Each point and vertical bar represent the mean ± S.D. of 4 determinations.

**Fig. 5 Effect of inhibitors of hepatic receptors and gene-knockout of *Lrpap1* on the hepatic and renal distribution of lanoteplase and t-PA in mice.**

After i.v. administration in normal mice of $^{125}$I-lanoteplase (A, C) or $^{125}$I-t-PA (B, D) at the dose of 1 μg/kg, the time-profiles of TCA-precipitable radioactivity in the plasma, and the radioactivity in the liver (A, B) and kidney (C, D) at 1, 2, 3 and 5 min were measured and are shown as integration plots (filled circles). The time profiles of radioactivity in plasma until 3 min, and radioactivities in the liver and kidney at 3 min

were also measured after i.v. administration under four different experimental conditions (difference in inhibitors or experimental animals): Those in the *lrpap1*$^{(-/-)}$ are shown as open circles, and those in the normal mice with co-administration of 120 μg/kg mannose, 180 μg/kg lactoferin or both 120 μg/kg mannose and 180 μg/kg lactoferin are shown as open squares, open triangles and open diamonds, respectively. The arrows indicate the data at 3 min after i.v. administration of $^{125}$I-lanoteplase or $^{125}$I-t-PA alone in the normal mice. The asterisks represent significant difference in Kp values as compared with that in the normal mice at 3 min after i.v. administration (*$p<0.05$, **$p<0.01$).

DMD Fast Forward. Published on December 18, 2006 as DOI: 10.1124/dmd.106.012518
This article has not been copyedited and formatted. The final version may differ from this version.



## Tables

Table 1 Kinetic parameters of the RME of lanoteplase and t-PA[a)]

| | $k_{off}$ ($min^{-1}$) | $k_{int}$ ($min^{-1}$) | $k_{deg}$ ($min^{-1}$) |
|---|---|---|---|
| Lanoteplase | 0.050±0.001 | 0.148±0.018 | 0.036±0.009 |
| t-PA | 0.015±0.029 | 0.281±0.029 | 0.100±0.016 |

a) Each parameter was calculated based on the data shown in Fig. 5, and expressed as mean ± calculated SD.

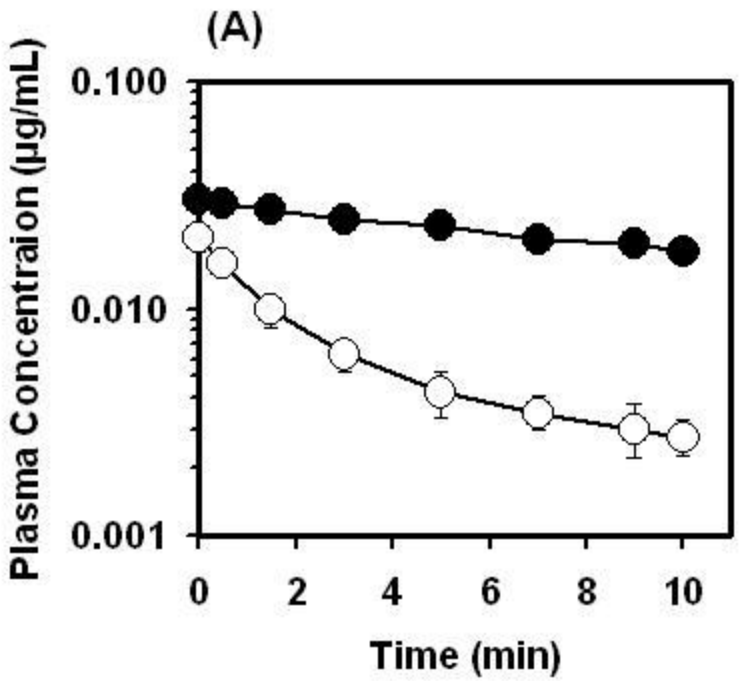


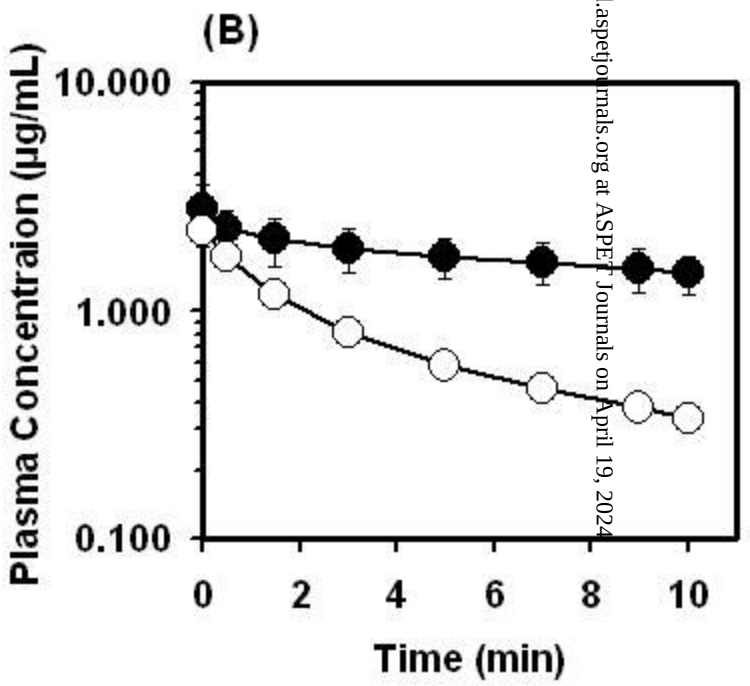




Fig. 1

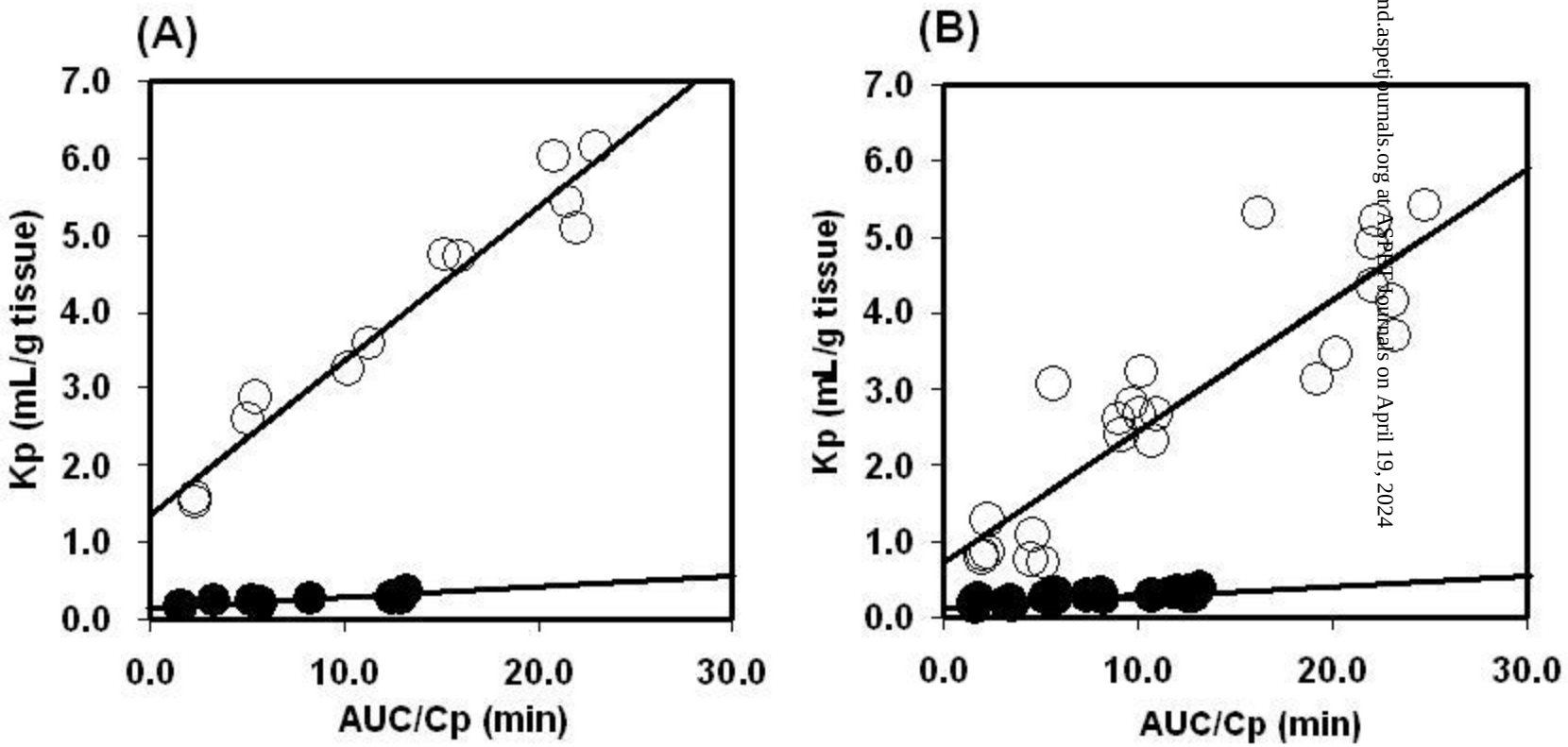




Fig. 2

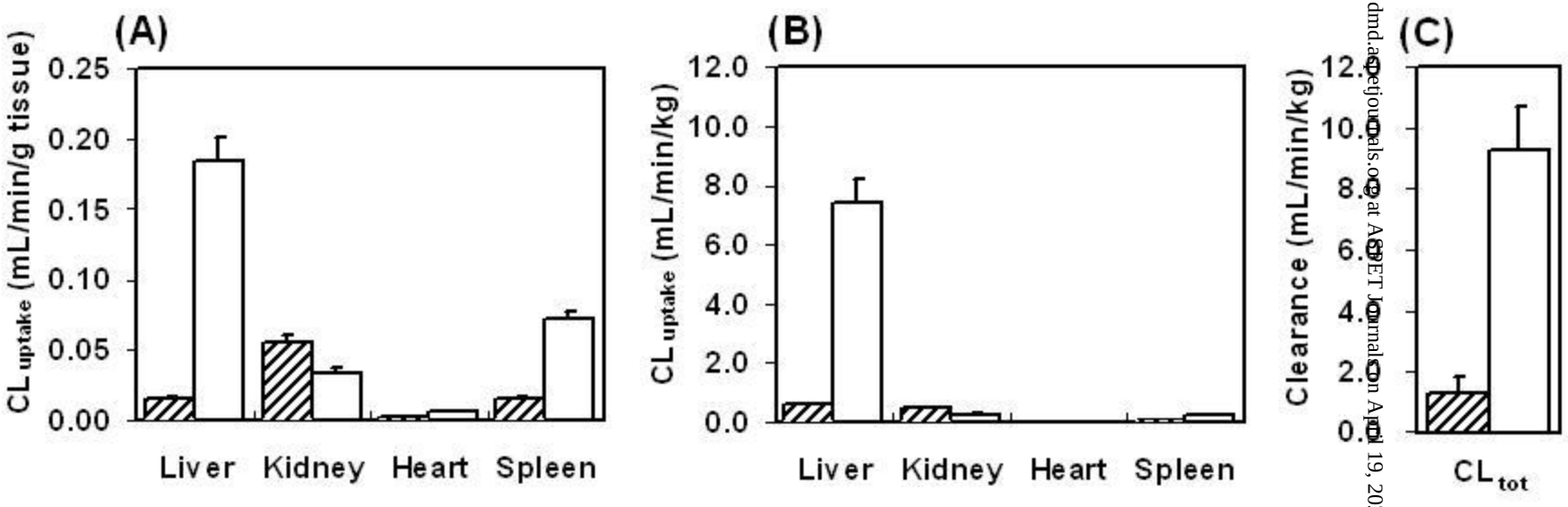


Fig. 3

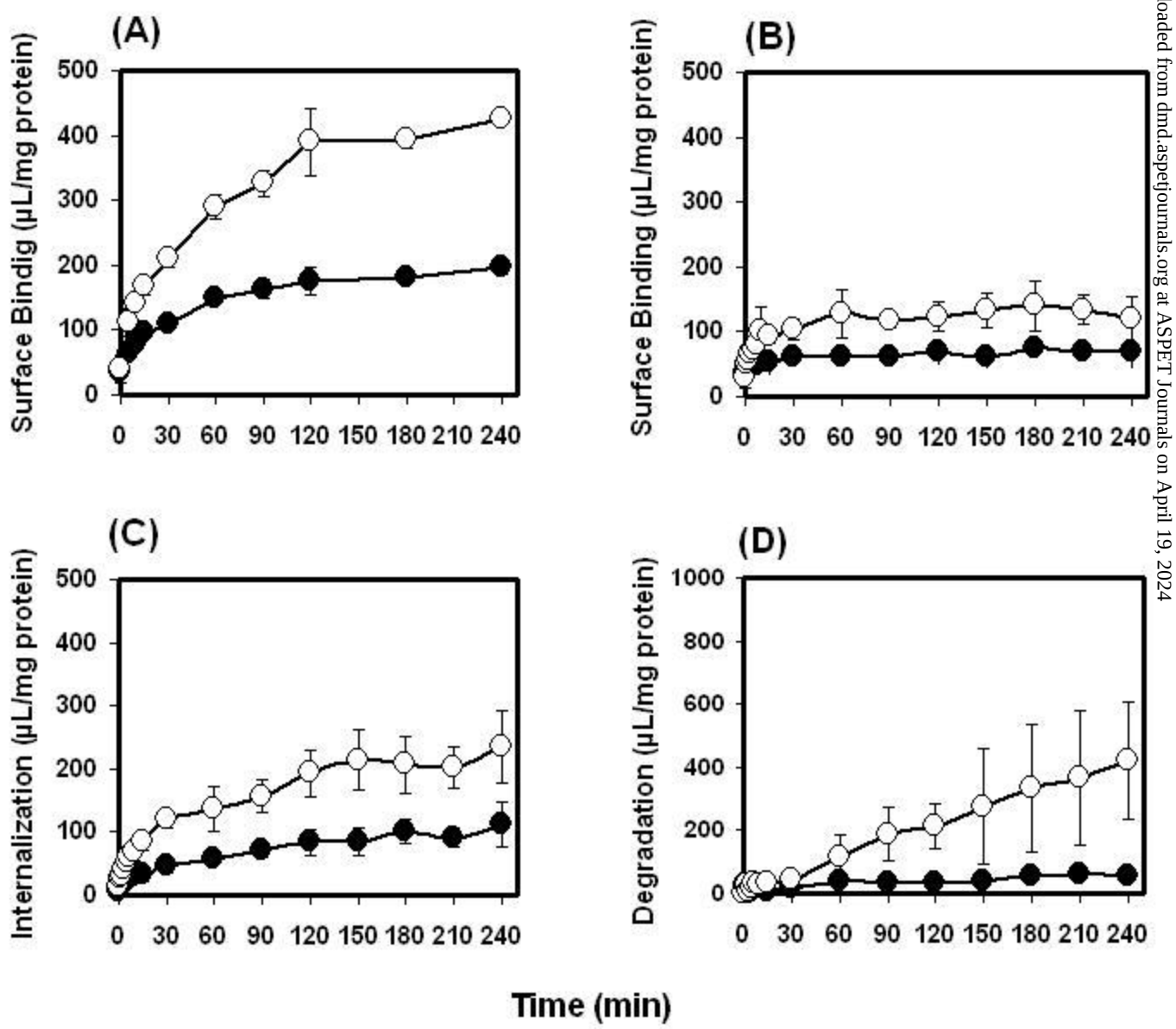


Fig. 4

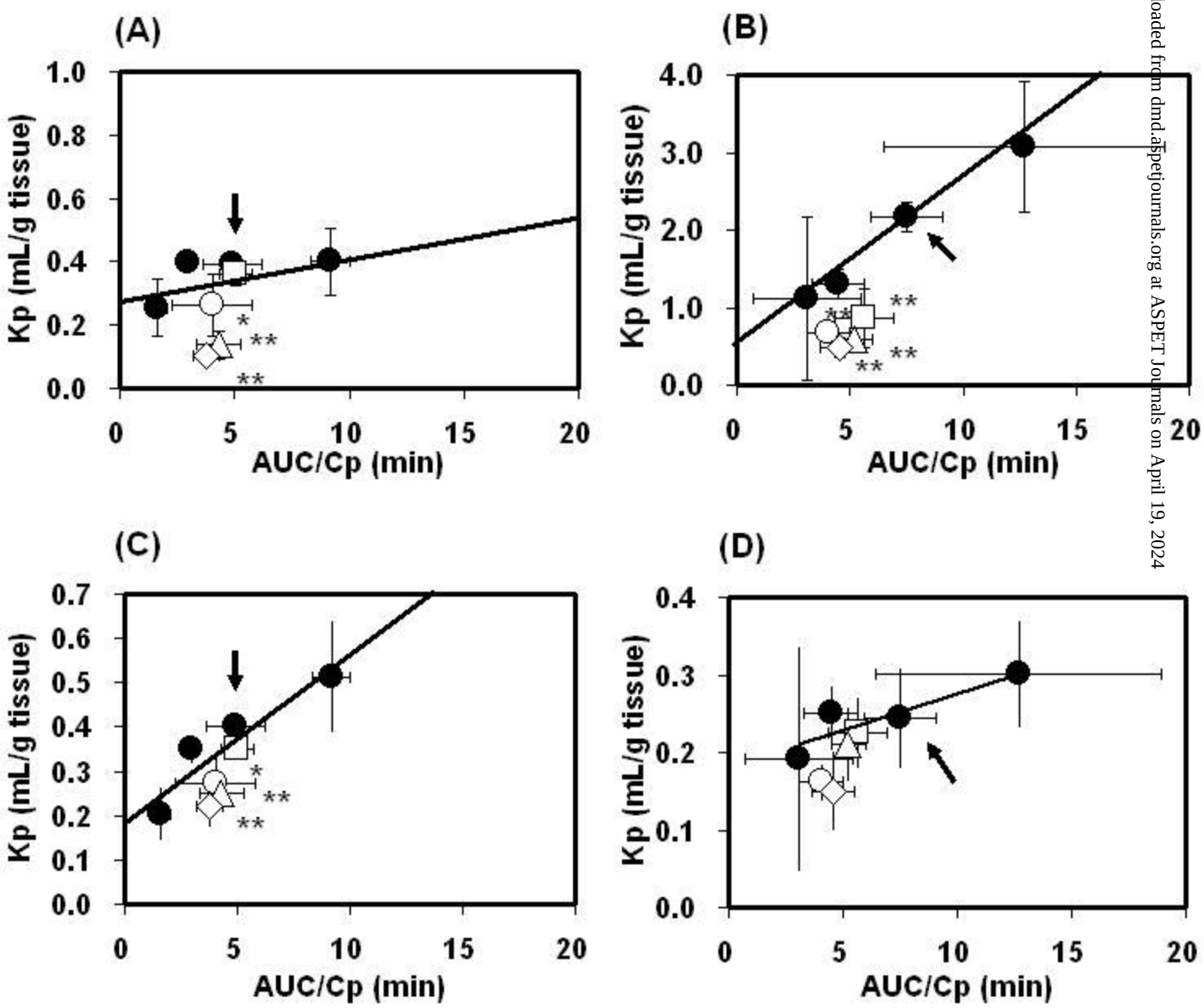




Fig. 5